Environmental Research 159 (2017) 164–175

Contents lists available at ScienceDirect

Environmental Research

journal homepage: www.elsevier.com/locate/envres

The effect of aluminium and sodium impurities on the in vitro toxicity and pro-inflammatory potential of cristobalite

C. Nattrass[a], C.J. Horwell[a,*], D.E. Damby[b,c], D. Brown[d], V. Stone[d]

[a] Institute of Hazard, Risk & Resilience, Department of Earth Sciences, Durham University, Durham DH1 3LE, UK
[b] Department of Earth and Environmental Sciences, Ludwig-Maximilians-Universitaet Muenchen, Munich 80333, Germany
[c] United States Geological Survey, Menlo Park, California 94025, USA
[d] School of Life Sciences, Heriot-Watt University, Edinburgh EH14 4AS, UK

ARTICLE INFO

Keywords:
Cristobalite
Crystalline silica
Cytotoxicity
Haemolysis
Impurities

ABSTRACT

Background: Exposure to crystalline silica (SiO_2), in the form of quartz, tridymite or cristobalite, can cause respiratory diseases, such as silicosis. However, the observed toxicity and pathogenicity of crystalline silica is highly variable. This has been attributed to a number of inherent and external factors, including the presence of impurities. In cristobalite-rich dusts, substitutions of aluminium (Al) for silicon (Si) in the cristobalite structure, and impurities occluding the silica surface, have been hypothesised to decrease its toxicity. This hypothesis is tested here through the characterisation and in vitro toxicological study of synthesised cristobalite with incremental amounts of Al and sodium (Na) dopants.

Methods: Samples of synthetic cristobalite with incremental amounts of Al and Na impurities, and tridymite, were produced through heating of a silica sol-gel. Samples were characterised for mineralogy, cristobalite purity and abundance, particle size, surface area and surface charge. In vitro assays assessed the ability of the samples to induce cytotoxicity and TNF-α production in J774 macrophages, and haemolysis of red blood cells.

Results: Al-only doped or Al + Na co-doped cristobalite contained between 1 and 4 oxide wt% Al and Na within its structure. Co-doped samples also contained Al- and Na-rich phases, such as albite. Doping reduced cytotoxicity to J774 macrophages and haemolytic capacity compared to non-doped samples. Al-only doping was more effective at decreasing cristobalite reactivity than Al + Na co-doping. The reduction in the reactivity of cristobalite is attributed to both structural impurities and a lower abundance of crystalline silica in doped samples. Neither non-doped nor doped crystalline silica induced production of the pro-inflammatory cytokine TNF-α in J774 macrophages.

Conclusions: Impurities can reduce the toxic potential of cristobalite and may help explain the low reactivity of some cristobalite-rich dusts. Whilst further work is required to determine if these effects translate to altered pathogenesis, the results have potential implications for the regulation of crystalline silica exposures.

1. Introduction

Crystalline silica, in the form of quartz, tridymite or cristobalite, can cause respiratory diseases when inhaled, such as silicosis (Greenberg et al., 2007; Leung et al., 2012), and is listed as a carcinogen by the International Agency for Research on Cancer (IARC, 1997). However, crystalline silica toxicity has been described as 'a variable entity' (Donaldson and Borm, 1998), as it has variable fibrogenic, mutagenic and carcinogenic potency (Donaldson and Borm, 1998; Meldrum and Howden, 2002; Mossman and Glenn, 2013). The variable toxicity of crystalline silica has been attributed to both the inherent characteristics of the silica particle and external factors that can alter the particle surface reactivity (IARC, 1997), including the presence of impurities (Fubini, 1998).

Quartz is the most common form of crystalline silica, however, exposure to cristobalite is also common in some industries, such as the diatomaceous earth industry where processed samples can contain up to 85 wt% cristobalite (e.g., Bye et al., 1984, Rafnsson and

Abbreviations: PVNO, Polyvinyl pyridine N-oxide; XRF, X-ray fluorescence; EMPA, Electron microprobe analysis; XRD, X-ray diffraction; SEM, Scanning electron microscopy; EDS, Energy dispersive X-ray spectroscopy; PIDS, Polarization intensity differentiation scattering; BET, Brunauer-Emmett-Teller; LDH, lactate dehydrogenase; TNF-α, Tumour necrosis factor alpha; OEL, Occupational exposure limit; PEL, Permissible exposure limit

* Corresponding author.
E-mail addresses: claire.nattrass191@hotmail.co.uk (C. Nattrass), claire.horwell@durham.ac.uk (C.J. Horwell), ddamby@usgs.gov (D.E. Damby), d.brown@hw.ac.uk (D. Brown), v.stone@hw.ac.uk (V. Stone).

http://dx.doi.org/10.1016/j.envres.2017.07.054
Received 10 April 2017; Received in revised form 24 July 2017; Accepted 31 July 2017

Gunnarsdóttir, 1997). In environmental settings, substantial quantities of cristobalite have been found in volcanic ash, such as from the 1980 Mount St Helens, USA eruption (Damby, 2012; Dollberg et al., 1986), and the sustained eruptions of Soufrière Hills Volcano, Montserrat, which produced volcanic ash containing up to 25 wt% cristobalite (Horwell et al., 2014).

The open crystal structure of cristobalite, compared to quartz, readily allows for the incorporation of other elements into the structure through substitutions of cations into the silica tetrahedra (Deer et al., 2013). Analyses of volcanic and diatomaceous earth cristobalite samples, by the authors, have shown that they always contain impurities. In volcanic cristobalite, this is predominantly Al and Na (up to 4 oxide wt % combined) (Horwell et al., 2012). In diatomaceous earth cristobalite, Al, Fe, Na, and Ca have been observed (Nattrass et al., 2015) (up to 13 wt% combined (Nattrass, 2015)). The incorporation of these elements into the crystal structure is likely due to the substitution of Al^{3+} or Fe^{3+} for Si^{4+} and with interstitial Na^{+} or Ca^{2+} to balance the charge (Deer et al., 2013).

As with quartz, toxicology studies have shown that cristobalite can increase gene expression and cytokine release in macrophage and lung epithelium models (Perkins et al., 2012; Barrett et al., 1999), as well as trigger inflammasome activation (Peeters et al., 2014; Damby et al., 2015). However, cristobalite exposure in pottery workers did not appear to cause any adverse effects (Cherry et al., 1998), cristobalite-rich volcanic ash has low toxicity in vitro (Damby et al., 2016; Wilson et al., 2000) and in vivo (Cullen et al., 2002; Housley et al., 2002) and, clinically, there is currently no evidence of chronic disease from exposure to volcanic ash (Baxter et al., 2014). In diatomaceous earth workers, the evidence is conflicting; a number of epidemiology studies have attributed increased mortality (Checkoway et al., 1993), lung cancer (Rice et al., 2001) and other lung diseases (Park et al., 2002) to cristobalite exposure. This has been supported clinically (Hughes et al., 1998), however, some studies of different cohorts show no significant increase in lung disease (Rafnsson and Gunnarsdóttir, 1997) and opacities dissimilar to those of silicosis (Harber et al., 1998; Vigliani and Mottura, 1948). Toxicology studies have found cristobalite-rich diatomaceous earth to have low cytotoxicity and pro-inflammatory potential (Nattrass et al., 2015; Bye et al., 1984; Ghiazza et al., 2009), and no fibrotic effect on rats, guinea-pigs or dogs (Wagner et al., 1968). That epidemiology and toxicology studies of impure, occupational or naturally-occurring cristobalite generally show a lower toxicity, compared to toxicology studies of pure cristobalite powders, suggests impurities may play a role in altering cristobalite toxicity.

It has been hypothesised that structural substitutions can inhibit the toxicity of cristobalite in a similar way to treating the crystalline silica surface (Horwell et al., 2012; Nattrass et al., 2015). Treatment of a quartz surface with Al lactate or polyvinyl pyridine N-oxide (PVNO) has been shown to dampen its cytotoxicity, haemolytic potential and ability to damage DNA (Duffin et al., 2001; Knaapen et al., 2002; Stone et al., 2004; Nolan et al., 1981). Treatment with Fe has led to inconclusive results, in some cases causing an increase in reactivity, in others no change and in some cases a reduction in toxicity (Cullen et al., 1997; Fubini et al., 1995). In mixed dusts containing crystalline silica, such as volcanic ash or coalmine dust, the presence of other mineral and amorphous phases can occlude the silica particle surface (Donaldson and Borm, 1998; Ghiazza et al., 2009; Horwell et al., 2012; Tourmann and Kaufmann, 1994), and may also interact with the silica surface, as clay extracts have been shown to dampen quartz toxicity (Stone et al., 2004).

Due to confounding factors, such as the presence of other mineral particles and variations in particle size and surface area within and among samples, the role of structural substitutions in controlling the toxicity of cristobalite dusts has not yet been determined. It is important to establish whether the structural makeup of cristobalite is capable of influencing its pathogenic potential so that these data can be taken into account in risk assessment, and, eventually, exposure regulations in cristobalite industries. Therefore, the aim of this study was to determine if structural impurities in cristobalite can alter its toxic potential. Rather than comparing a range of natural samples of uncontrolled composition, we instead assessed the in vitro toxicity of synthetic cristobalite samples with structural impurities introduced by systematic doping with incremental amounts of Al, with and without Na.

2. Materials and methods

2.1. Materials

Crystalline silica with and without impurities was produced using a silica sol-gel method adapted from Chao and Lu (2002b). Colloidal silica sol (Ludox TM-40, Sigma Aldrich) was dried at 120 °C for at least 12 h, in its pure form, or with dopants added. Samples were doped with Al and Na nitrates in equivalent concentrations of 1, 2 and 3 wt% Al_2O_3 in a 1:1 M ratio of Al to Na, while accounting for the Al and Na already in the silica sol, as measured by X-ray fluorescence (XRF; data in Additional file 1). The concentration range was defined in order to understand the effect of sequentially increasing Al and Na impurity contents, in accordance with abundances observed in natural cristobalite (Horwell et al., 2012). One Al-only doped sample was also produced to constrain the role of Al, where only 3 wt% Al_2O_3 (and no additional Na) was added to the starting material.

The resultant dried cakes were gently ground by hand and 5 g pressed into 32 mm diameter pellets at a pressure of 120 MPa, using a uniaxial press. Pellets were then heated at 1100 °C in a Carbolite horizontal tube furnace (Durham University; Table 1) at a rate of 4.4 °C/min and held at the target temperature for 24 h, before being cooled at the rate of the furnace. Synthesis experiments could not be conducted in the cristobalite stability field (> 1470 °C (Deer et al., 2013)) because doped samples treated at > 1300 °C melted, due to the decreased eutectic temperature imparted by the impurities. Therefore, a synthesis temperature of 1100 °C was selected as it is partway between the melting temperature and the upper limit of quartz stability (870 °C (Deer et al., 2013)). Further, naturally-occurring and industrial cristobalites are produced metastabily at, or below, this temperature in the exposure settings of interest, such as the diatomaceous earth industry and volcanic environments (Horwell et al., 2013; Engh, 2000), and this temperature was appropriate, therefore, from both experimental and exposure perspectives.

Table 1
Sample production conditions (treatment temperature, time, dopant concentrations), and sample mineralogy (XRD and SEM-EDS).

	Sample name	Furnace conditions		Dopants added (oxide wt%)		Minerals (trace)*
		Temp (°C)	Time (h)	Al	Na	
Non-doped	1600_12	1600	12	0.0	0.0	Cristobalite
	1600_4	1600	4	0.0	0.0	Cristobalite
	1100_24	1100	24	0.0	0.0	Tridymite, (cristobalite)
Doped	2Al + Na	1100	24	1.0	0.6	Cristobalite, (albite, ?)
	3Al + Na	1100	24	2.0	1.2	Cristobalite, albite, ?
	5Al + Na	1100	24	3.0	1.8	Cristobalite, albite, ?
	3Al	1100	24	3.0	0.0	Cristobalite, (albite, ?)
Raw materials	SS	–	–	0.0	0.0	–
	5Al + Na_SS	–	–	3.0	1.8	–

? represents unidentified phase.
* Phases in parentheses were only observed in trace quantities.

Table 2
Cristobalite abundance, cristobalite primary XRD peak position, and cristobalite chemistry of samples.

	Samples	Cristobalite abundance (% ± s.d.)	Cristobalite primary peak position (° 2θ ± s.d.)	Cristobalite chemistry (wt% ± s.d.)		
				SiO_2	Al_2O_3	Na_2O
Non-doped	1600_12	92 ± 4	21.95 ± 0.02	99.9 ± 0.4	0.0 ± 0.0	0.1 ± 0.1
	1600_4	87 ± 8	21.96 ± 0.04	99.6 ± 0.4	0.0 ± 0.0	0.1 ± 0.1
	1100_24	NA	NA	NA	NA	NA
Doped	2Al + Na	88 ± 9	21.94 ± 0.03	98.4 ± 0.7	0.7 ± 0.3	0.5 ± 0.2
	3Al + Na	64 ± 9	21.89 ± 0.04	97.6 ± 1.1	1.4 ± 0.7	0.8 ± 0.4
	5Al + Na	63 ± 20	21.79 ± 0.03	95.9 ± 2.0	2.5 ± 1.2	1.4 ± 0.6
	3Al	59 ± 3	21.87 ± 0.05	NA	NA	NA

Cristobalite abundance (peak area by XRD (n = 2)), cristobalite primary XRD peak position (n = 2; indicative of structural impurities), and cristobalite chemistry (EMPA (n > 30)). s.d. = one standard deviation; NA = not analyzed. Raw materials contained no cristobalite so data are not included in the Table.

For comparison, non-doped pellets were also heated for 4 or 12 h at 1600 °C (Table 1), above the tridymite-cristobalite transition temperature (Deer et al., 2013), to produce a non-doped cristobalite with a level of crystallinity more similar to the doped samples (Table 2) and a highly-crystalline non-doped cristobalite, respectively. The starting material (silica sol; SS), dried at 120 °C and ground by hand, with 5 wt % total Al + Na (5Al + Na_SS) and without dopants, were also tested pre-crystallisation, as non-crystalline material controls. Samples and their preparation conditions are presented in Table 1.

A slice of each pellet was mounted as polished resin blocks and coated with 16 nm carbon for analysis by electron microprobe analyzer (EMPA). The rest of each pellet was crushed with an agate pestle and mortar and then ground in a cryogenic mill (to avoid any impact of sample heating on crystallinity) in air at 12 cycles per second for 30 min, to produce a powder. Toxicological assays were conducted on the milled material which was not further chemically digested to isolate the cristobalite, as this is known to alter the crystalline silica surface and reactivity (Fubini, 1998).

2.2. Particle characterisation

The mineralogy of the samples was determined by X-ray diffraction (XRD) using a Bruker AXS D8 ADVANCE with DAVINCI design (Durham University). Sub-samples of the cryogenically-milled pellets were further ground, using an agate pestle and mortar, sieved onto silicon discs to ensure random orientation, and identification of phases was performed using a locked-coupled scan from 2 to 90° 2θ with an 8 h scan time. Mineral identification was performed by comparison with library patterns (ICDD, 2015). Ground samples were also compacted into a deep well mount using the knife-edge of a spatula to ensure random crystal orientation (Batchelder and Cressey, 1998). A run was then performed using a fixed parallel beam (6° θ) and a moving detector to cover the range 18–35° 2θ, allowing the abundance of cristobalite to be determined by peak-area measurements of the primary cristobalite peak (~21.8° 2θ), and accurate measurements of primary cristobalite peak position (an indicator of crystal purity (Damby et al., 2014)) to be obtained.

The chemical composition of cristobalite was measured on cross sections of a sub-sample of each pre-ground pellet by EMPA, using a Cameca SX100 (Ludwig Maximilian University of Munich). A voltage of 15 kV and current of 4 nA was applied to measure Na, Al and Si concentrations. For Fe, Mg, K and S (present in the resin) concentrations, a 40 nA current was used (see Additional file 1). Areas for analysis were selected by the characteristic cracking indicative of cristobalite at room temperature that has undergone the β to α transition (Carpenter et al., 1998). Backscatter imaging by scanning electron microscopy (SEM) and energy dispersive X-ray spectroscopy (EDS) mapping was also performed, at 15 kV (Hitachi SU-70 FEG SEM, Durham University), to identify chemically-distinct phases in the sectioned pellet.

Particle size distributions were analysed by laser diffraction using a Coulter LS analyser (Durham University), with polarization intensity differentiation scattering (PIDS). Particles were suspended in water until an obscuration value of 8–12% was acquired, and sonicated for 120 s prior to analysis. Data were analysed by Fraunhofer theory and are presented as the cumulative volume %, volume % and median diameter. Particle size was also qualitatively assessed by SEM imaging using a Hitachi SU-70 FEG-SEM with a voltage of 8 kV (Durham University).

Specific surface area was analysed by nitrogen adsorption measurements at 77 K using a TriStar 3000 instrument (Durham University). Samples were dried in nitrogen gas at 120 °C overnight. The Brunauer-Emmett-Teller (BET) theory was applied to measurements at relative pressures of 0.05–0.24, and the results are the mean of three repeated measurements.

Zeta potential measurements were performed to determine particle surface charge, which has been shown to be an important factor in the cytotoxicity of silica nanoparticles to keratinocytes (Park et al., 2013). Samples at 62.5 μg/ml in complete medium (RPMI medium, containing 10 μl/ml L-glutamine, 10 μl/ml penicillin and streptomycin, and 10% foetal bovine serum, pH 7) were sonicated for 20 min and the zeta potential measured using a Malvern Nanosizer (Heriot Watt University).

2.3. Toxicology

Cytotoxicity of the samples towards J774 macrophages was measured using the alamarBlue® and WST-1 assays (both a measure of metabolic capacity), and the lactate dehydrogenase (LDH; a measure of cell membrane damage) assay. Macrophages were chosen as they are phagocytes and are actively involved in particle clearance from the lung. Toxicity to these cells will result in reduced clearance and, therefore, potential biopersistence of insoluble particles. Further, sub-lethal activation can promote inflammation. Therefore, macrophages play a key role in the physiological and pathophysiological responses to inhaled particles, and use of well-established model cell lines, like J774, allows for testing of this response. Samples were suspended in complete medium and sonicated for 20 min at 37 °C at 50–50 Hz (Ultrawave Q; Heriot Watt University). J774 macrophages were seeded in a 96 well plate (5×10^4 cells per well) and exposed to 100 μl of particle suspension in concentrations of 8, 16, 31, 62, 125, 250, and 500 μg/ml for 24 h or 48 h at 37 °C and 5% CO_2. Following exposure, the supernatant was removed and stored at −80 °C for LDH and cytokine analysis. For the alamarBlue® assay, a solution of 1 mg/ml alamarBlue® reagent (resazurin sodium salt; Sigma) in saline was diluted 1:10 in complete medium and 100 μl added to the cells. The plate was incubated for 4 h and fluorescence measured with excitation at 560 nm and emission at 590 nm. For the WST-1 assay, cells were exposed to sample treatments in the same way for 24 h, the supernatant was removed from the cells and 100 μl WST-1 (tetrazolium salt; Roche), diluted 1:10 in complete medium, was added to each well. Cells were incubated for 3 h and the

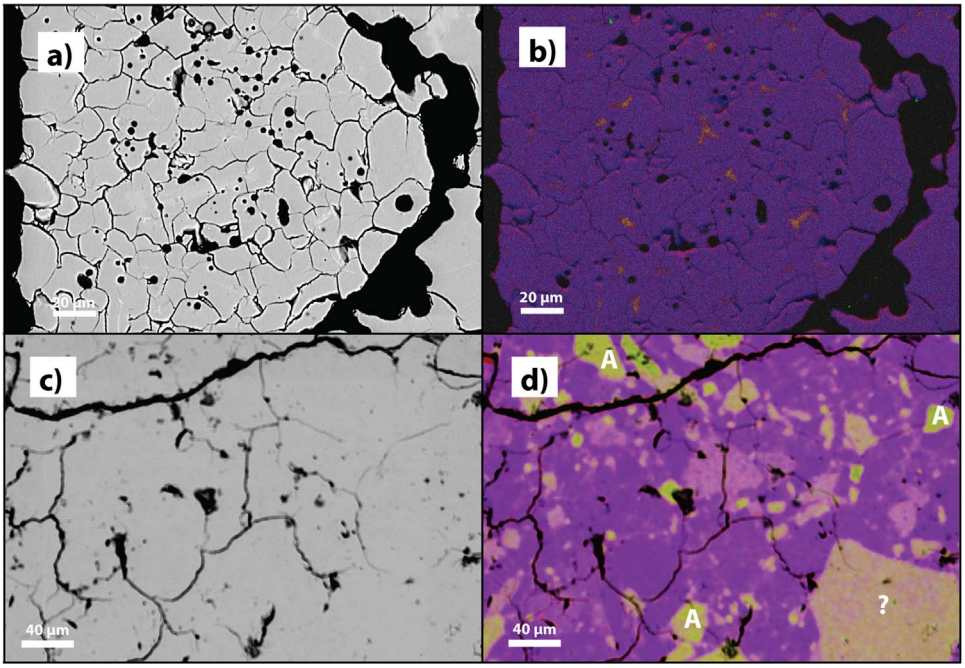

Fig. 1. Backscatter images and chemical composition maps of sectioned samples. Chemical composition maps (blue = Si, red = O, yellow = Na, green = Al) measured by energy dispersive X-ray spectroscopy (EDS) of sectioned **a-b)** non-doped 1600_12 and **c-d)** doped 5Al + Na samples. A = albite, ? = unidentified Al- and Na-rich silicate. (For interpretation of the references to color in this figure legend, the reader is referred to the web version of this article.)

absorbance measured at 450 nm. LDH release from macrophages was measured by adding 10 µl of cell supernatant to 50 µl 1 mg/ml NADH in 0.75 mM sodium pyruvate, incubating for 30 min at 37 °C in 5% CO_2, adding 50 µl of 2 mg/ml 2,4-dinitrophenylhydrazine in 1 M HCl and incubating for 20 min at room temperature in the dark, before adding 50 µl 4 M sodium hydroxide and measuring the absorbance at 550 nm. Imaging of untreated and particle-treated cells post-24 h exposure was performed using light microscopy to qualitatively assess particle uptake and cell viability.

Leachate solutions were also assessed by the alamarBlue® assay, to constrain the contribution of soluble components to observed reactivity. Particle suspensions at 500 µg/ml (the top concentration tested) in complete medium were incubated for 24 h and centrifuged at 10,000 × *g* for 10 min to remove particles. The leachate was then used in the alamarBlue® assay at 24 h exposure.

Tumour necrosis factor alpha (TNF-α) was measured as a marker of inflammation, as TNF-α is a pro-inflammatory cytokine associated with silica-induced toxicity (Mossman and Glenn, 2013; Piguet et al., 1990). TNF-α was measured in the supernatant of cell cultures treated with 125, 62, or 16 µg/ml of the samples for 4 and 24 h, to capture initial TNF-α production, and levels at the first time point of measured cytotoxicity, respectively, using BD™ Cytometric Bead Array cytokine flex sets (BD Biosciences) according to the manufacturer's instructions.

Haemolysis was used to measure the ability of particles to rupture cell membranes, and has been shown to be a good indicator of the pro-inflammatory potential of crystalline silica (Pavan et al., 2014). A volume of 1 ml of sheep blood in Alsever's solution (Oxoid Ltd.) was centrifuged at 2348 × *g* for 2 min and the supernatant removed. Isolated red blood cells were washed three times with saline and 100 µl of cells were added to 3.6 ml saline. Particle suspensions of 1 mg/ml particles in saline were sonicated for 20 min, serially diluted to final concentrations of 1000, 500, 250, 125 and 62 µg/ml, and 150 µl of the particle suspensions added to 96 well plates in triplicate. Next, 75 µl of the prepared blood was added to each well, the plate covered and placed on an orbital shaker for 1 h. Post-exposure, the plate was centrifuged at 250 × *g* for 5 min, 100 µl of the supernatant was transferred to a new plate and absorbance measured at 540 nm.

In all assays, 0.5% Triton-X in either complete medium or saline was used as a positive control and untreated cells as a negative control. DQ12, a quartz sand with high toxic potency and < 5 µm in diameter, was used as a high-toxicity crystalline silica standard and TiO_2 (Degussa; 25 nm particle size) as a low-toxicity particle standard.

2.4. Statistical analyses

ANOVA general linear model with a Tukey's post-hoc test was performed to determine the significance of differences among samples in the in vitro assays (Minitab 15; * $p < 0.05$, ** $p < 0.01$, *** $p < 0.001$).

3. Results

3.1. Particle characterisation

Cristobalite constituted ~90% of both the non-doped samples heated at 1600 °C (1600_12 and 1600_4) and the doped sample 2Al + Na, while cristobalite contributed ~60% of samples doped with > 3 oxide wt% Al or Al + Na (Table 1 and Table 2). The non-doped sample heated at 1100 °C (1100_24) contained substantial quantities of tridymite (another crystalline silica polymorph), and cristobalite content could not be determined due to peak overlap in the XRD patterns (Table 1). By SEM, the sample appeared to be predominantly tridymite, as it did not contain the characteristic cracking of cristobalite. Elemental analysis by electron microprobe on selected cristobalite areas showed that the Al and Na content in cristobalite increased as the amount of dopant was increased (Table 2). A shift in the cristobalite primary XRD peak towards lower 2θ values as dopant concentration increased was observed (Table 2). This is indicative of increased d-spacing (a measure of the unit cell size in the crystal), which has been attributed to the presence of impurities within the crystal structure (Damby et al., 2014).

Albite ($NaAlSi_3O_8$), a feldspar, was observed in small amounts in the XRD patterns of 3Al + Na, 5Al + Na, and in trace quantities in 2Al + Na and 3Al, as these were only detected in long duration XRD scans. Other Al- and Na-rich crystals, enriched in Si compared to albite but otherwise similar in chemistry, were observed in all Al + Na doped samples by SEM-EDS (Fig. 1) but were not detected by XRD and could not be identified. Albite or Al- and Na-rich minerals were not detected in non-doped samples (Fig. 1b). Amorphous material constituted the remainder of each sample, and amorphous content was greater in doped samples compared to non-doped samples.

For particles generated for the toxicological assays, by volume %,

Table 3
Physical characteristics and surface charge measurements of samples.

	Sample	Median particle diameter (μm)	Surface area		Surface charge	
			(m^2/g)	s.d.	(mV)	s.d.
Non-doped	1600_4	7.3	4.0	0.1	−11.4	0.8
	1600_12	10.9	0.9	0.1	−9.8	1.1
	1100_24	8.9	4.0	0.5	−11.1	0.6
Doped	2Al + Na	7.4	2.1	0.2	−9.8	0.8
	3Al + Na	6.4	4.7	0.0	−10.7	1.1
	5Al + Na	6.6	2.7	0.1	−10.0	0.8
	3Al	6.0	4.9	0.2	−10.7	1.2
Raw materials	SS	NA	94.6	2.8	−9.5	0.8
	5Al + Na_SS	NA	87.0	0.8	−9.7	1.0
	DQ12	NA	9.2	0.2	−10.5	0.8
	TiO_2	NA	NA	NA	−9.8	1.4

Particle size (laser diffraction), surface area (BET) and surface charge in complete medium (RPMI + 10% foetal bovine serum + antibiotics; zeta potential) for non-doped and doped samples, starting material and standards. s.d. = one standard deviation. NA = not analyzed.

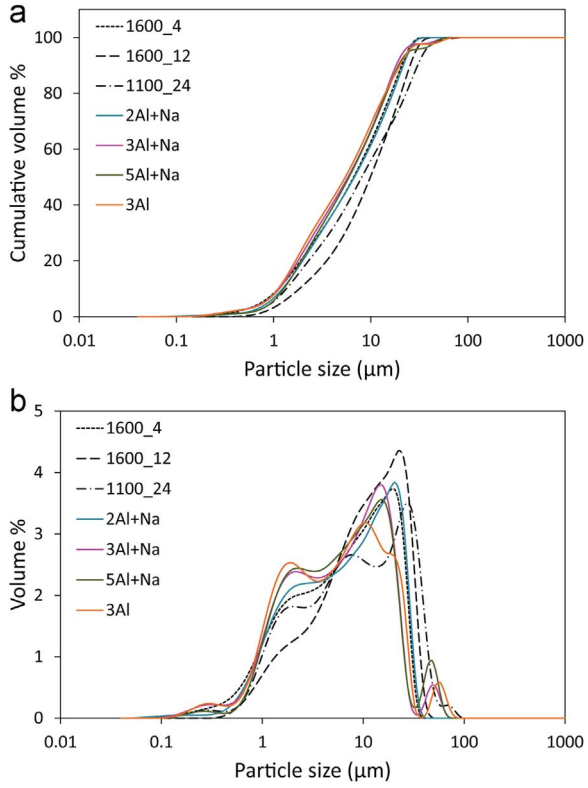

Fig. 2. Particle size distributions of crystalline silica samples. Particle size distributions of cryogenically-milled doped and non-doped crystalline silica samples measured by laser diffraction and presented as **a)** cumulative volume %, and **b)** volume %.

median particle diameter was between 5 and 7 μm for milled, doped samples and 1600_4 (Table 3). The other non-doped samples were slightly coarser, on average, with median diameters between 9 and 13 μm. All samples had > 90% particles < 30 μm in diameter (Fig. 2a), and had a bi- or multi-modal distribution (Fig. 2b). By SEM imaging, few particles were observed that were > 5 μm, indicating that, by number %, most particles were finer than the median indicated by laser diffraction (Fig. 3). Samples were sufficiently fine-grained for successful phagocytosis (Fig. 7).

Specific surface area ranged from 1 to 5 m^2/g in the synthesised samples, and was at least 19 times higher in the starting materials (Table 3). Surface charge of particles suspended in complete medium was between −9.5 and −11.4 mV for all samples and standards (Table 3).

3.2. In vitro toxicology assays

Cell viability was assessed using the alamarBlue®, WST-1 and LDH assays. Cell viability of J774 macrophages, measured by the alamarBlue® assay was sensitive to the positive control DQ12 quartz and not to the negative control TiO_2. A mixture of cytotoxicity results were observed for the non-doped samples, with 1100_24 and 1600_12 demonstrating significant decreases in viability at 24 h at the highest concentration tested (500 μg/ml), while 1600_4 did not. In addition, the cell viability at 48 h was significantly lower than 24 h for both non-doped 1600_4 and 1100_24, suggesting a time-dependent increase in toxicity. In contrast no significant toxicity was observed in the alamarBlue® assay for any doped samples at either time point or at any concentration compared to the control (Fig. 4). A small decrease in cell viability was observed at 48 h compared to 24 h for cells treated with 3Al doped sample (Fig. 4), but this effect is so small it is of little physiological relevance. Leachates and the starting materials (SS and 5Al + Na_SS) did not induce cytotoxicity in the J774 cells according to the alamarBlue® assay (data in Additional file 1).

Cell viability, measured by the WST-1 assay, generated unreliable data, possibly due to particle interference, and so are not presented.

The assessment of membrane damage via the LDH assay was performed after a 24 h exposure. Firstly, the positive control DQ12 induced significant cytotoxicity, while the negative control TiO_2 did not (Fig. 5). All synthesised samples induced a dose-dependent increase in LDH release. All three non-doped samples reached significant LDH release at concentrations of 250 μg/ml and higher (Fig. 5). In addition, the sample doped with 2Al + Na also displayed increased LDH release at exposure concentrations of 250 μg/ml and higher. In contrast, samples doped with 3Al, 3Al + Na or 5Al + Na only reached significant LDH release at exposure concentrations of 500 μg/ml. The data suggest that the 3Al doped sample was the least cytotoxic according to the LDH assay but, due to data variability, the effect of 3Al doped cristobalite was not statistically different from the other doped samples.

For the assessment of pro-inflammatory mediator production, the positive control DQ12 induced a dose-dependent increase in TNF-α production, while the negative control TiO_2 had no significant impact (Fig. 6). For the synthesised, doped and non-doped samples, no significant induction in TNF-α production by treated cells was observed compared to the untreated control at either 4 or 24 h exposure time (Fig. 6).

Light microscopy imaging of treated cells showed potential cellular uptake of particles from all samples, although it is possible particles were adhered to cell surfaces (Fig. 7). Some particles were clearly not engulfed, especially in cells treated with non-doped 1600_12 and 1100_24 samples.

Haemolysis is presented by mass and surface area dose (Fig. 8). As haemolysis is the direct interaction between the cell surface and particle surface it is appropriate to present the data as surface area dose, due to the variable surface area of the samples (Table 3). Firstly, DQ12, the positive control, induced dose-dependent haemolysis, while the negative control, TiO_2, had no significant effect. Sample-induced haemolysis was dose-dependent for all samples, except for those doped with 3Al + Na and 3Al, which were non-haemolytic at all concentrations tested (Fig. 8a). Non-doped 1100_24 was the most haemolytic sample, producing a similar dose response to the DQ12 positive control.

By surface area dose, the data do not fall on to one line, suggesting differences in the surface reactivity of the samples. The most potent samples, when expressed as surface area dose, were the synthesised, non-doped 1100_24 and the 1600_12. These were followed by DQ12 and the 2Al + Na doped sample which were almost identical, followed closely by the 5Al + Na doped sample and the non-doped 1600_4. Again, the 3Al + Na and 3Al doped samples did not induce a significant haemolytic effect when expressed as surface area dose (Fig. 8b).

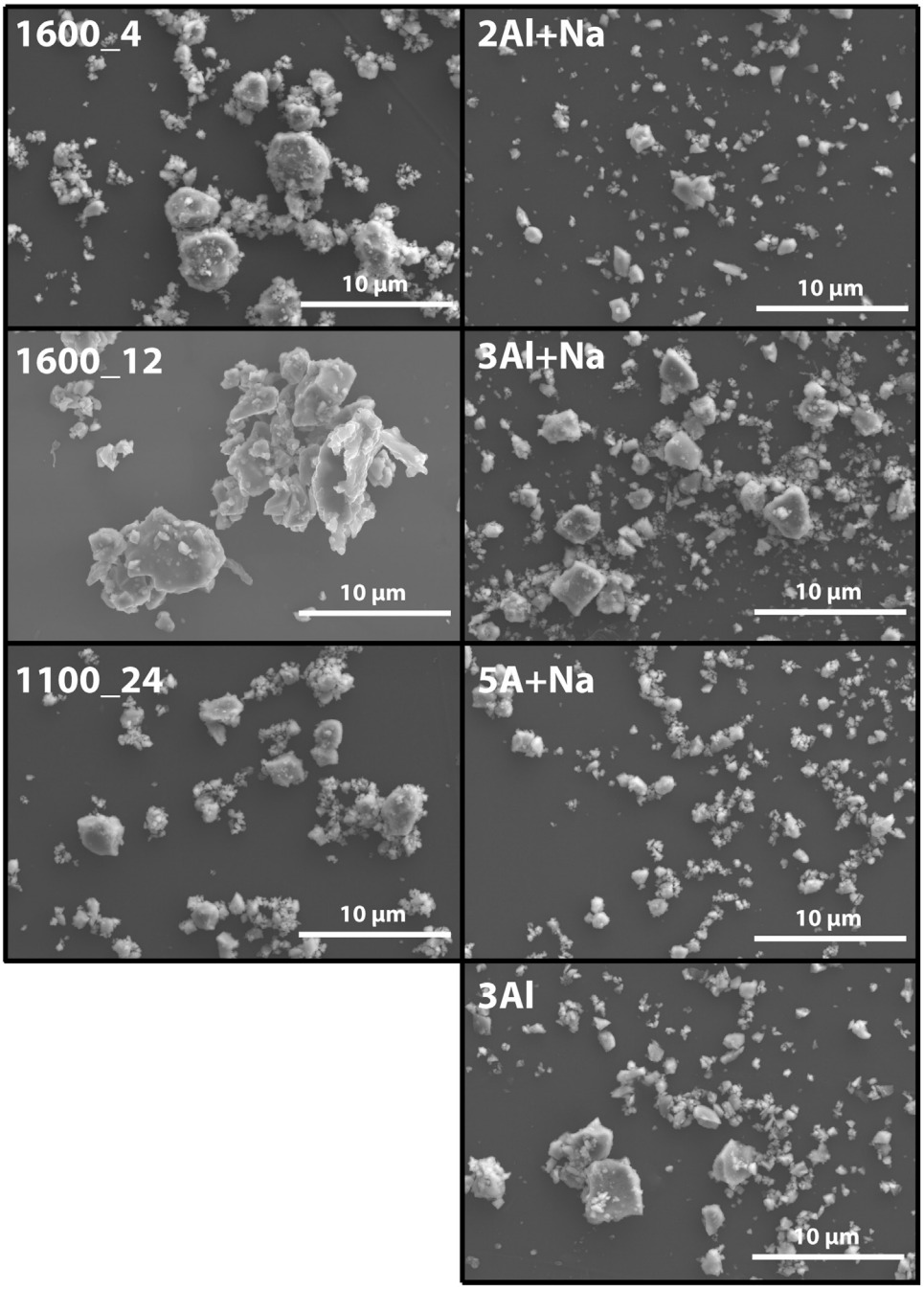

Fig. 3. Representative scanning electron microscopy images of synthetic crystalline silica particles.

4. Discussion

Chemical impurities have been identified as one potential factor which may affect the variable toxicity of crystalline silica (Donaldson and Borm, 1998). It has been hypothesised that structural Al impurities may have a similar dampening effect on the toxicity of naturally-impure cristobalite, such as that found in volcanic ash and processed diatomaceous earth (Horwell et al., 2012; Nattrass et al., 2015). However, no study, to date, has measured the effect of Al substitutions on cristobalite toxicity, directly. Here, the in vitro toxicity of cristobalite, synthesised to systematically vary concentrations of Al and Na dopants, was evaluated to determine whether chemical impurities can alter reactivity.

4.1. The effect of doping on crystalline silica toxicity in vitro

In general, when treating the J774 cell line in vitro, doping appeared to dampen cytotoxicity of the synthetic samples. This was most apparent in the LDH assay, and supported by the alamarBlue® assay, where only non-doped samples 1100_24 and 1600_12 elicited a significant cytotoxic response. The Al-only (3Al) doping seemed to be the most effective at preventing cytotoxicity in vitro, however, the difference between 3Al and the co-doped (Al + Na) samples was not statistically significant.

The magnitude of cytotoxicity varied by assay. The difference in sensitivity may be due to the nature of the endpoints which include a measure of metabolic capacity (alamarBlue® assay) versus a measure of membrane leakage (LDH assay), suggesting that membrane leakage could be occurring in cells where metabolic capacity is not suppressed. In both assays, the high-toxicity particle control (DQ12) gave a concentration-response relationship, as expected, and the low-toxicity particle control (TiO_2) had low toxicity, as expected, suggesting both assays were performed successfully. Interference of the particles in the

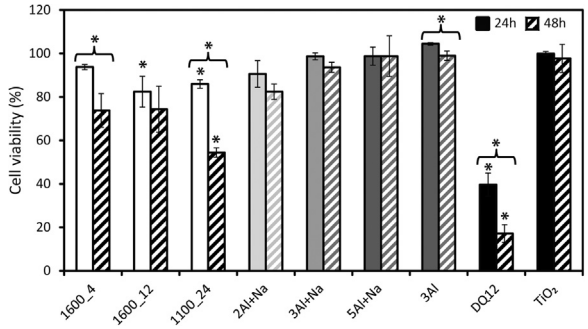

Fig. 4. Cell viability of J774 macrophages treated with crystalline silica samples measured by the alamarBlue® assay. Cell viability compared to an untreated control of J774 macrophages treated with 500 μg/ml non-doped samples (white), doped samples (grey), and standards (black) for 24 h (solid) or 48 h (striped). Error bars represent standard error (n = 4). * p = < 0.05 difference from untreated control, brackets indicate significant differences between exposure for 24 or 48 h.

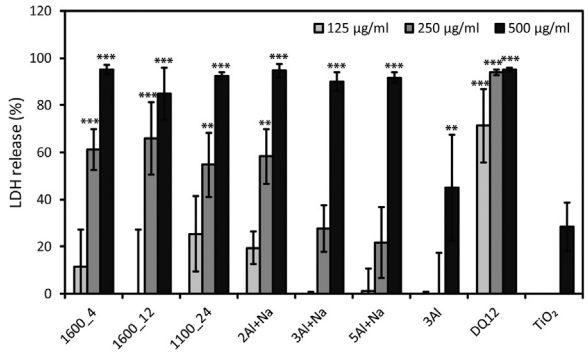

Fig. 5. Cytotoxicity of crystalline silica samples to J774 macrophages measured by the LDH assay. LDH release as a percentage of a positive (Triton-X) and untreated control for J774 macrophages treated with 125–500 μg/ml sample concentrations for 24 h. Error bars represent standard error (n = 4). ** p = < 0.01, *** p = < 0.001 difference from untreated control.

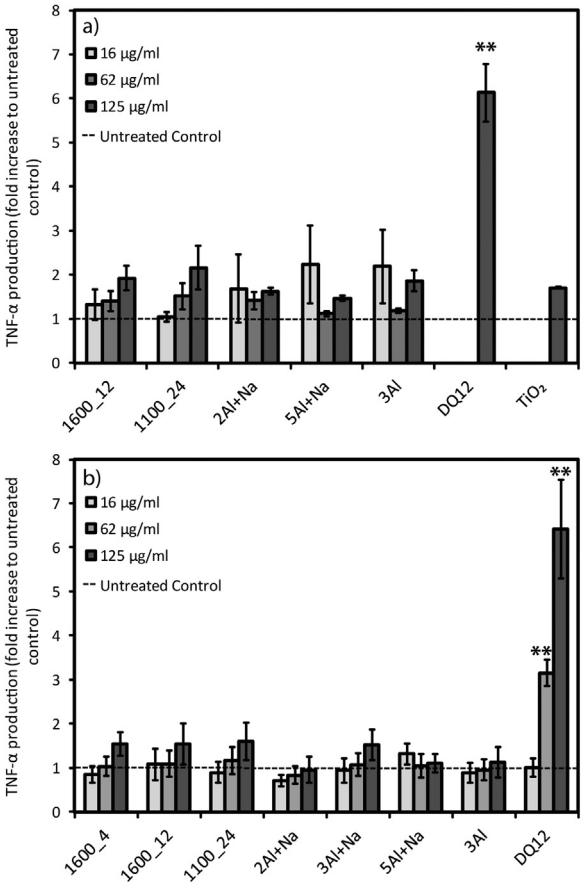

Fig. 6. TNF-α production by J774 macrophages exposed to crystalline silica samples. Exposures to concentrations of 16–125 μg/ml sample suspensions for **a)** 4, and **b)** 24 h. Error bars represent standard error (n = 3). ** p = < 0.01 difference from untreated control.

WST-1 assay, strengthens the argument for the use of multiple assays to assess cytotoxicity within a study of this type.

The haemolysis results also demonstrated differences among the potencies of the particles. The similarity in potency of the non-doped 1100_24 compared to the DQ12 positive control was clear when expressed as a mass dose, whereas doped samples (also produced at 1100 °C) were more than 28% less haemolytic at the top dose tested. Modifying the dose to the surface area metric suggested that the toxicity of 1600_12 sample, as well as 1100_24, was relatively high compared to DQ12, suggesting a more reactive particle surface than doped samples. In fact, doping with Al-only (3Al) eliminated the haemolytic potential altogether, supporting the hypothesis that doping decreased the haemolytic potential of the samples.

Regardless of the magnitude of toxicity, the same trend was observed in all assays: doping generally dampened particle reactivity. The potential mechanisms for this effect are now discussed.

4.2. Mechanisms of doping-induced suppression of crystalline silica toxicity

A primary mechanism by which doping likely reduces the toxicity of crystalline silica is by alteration of the particle surface which, in an insoluble particle, interacts with cells directly. Here, doping caused substantial changes in crystal chemistry through structural substitutions, affected crystalline silica abundance, degree of crystallinity and the polymorph formed, all of which can alter the particle surface properties, and, therefore, bioreactivity.

4.2.1. Chemical substitutions and structural impurities

The results of this study indicate that structural impurities in cristobalite reduce cytotoxicity and haemolytic ability. The Al-only doped sample (3Al) was consistently the least reactive (although not statistically different from samples doped with > 3 oxide wt% Al + Na) and, importantly, was the only doped sample (with > 3 oxide wt% dopant) not to have formed accessory minerals such as albite, the presence of which may influence toxicity (discussed below). It also had a similar cristobalite content to Al + Na doped samples. Therefore, there is strong evidence to suggest that the reduced cytotoxicity and haemolytic potential is caused by the addition of Al to the crystal structure, incorporation of which is evidenced by the shifted cristobalite XRD primary peak position compared to non-doped cristobalite.

Similarly, it is likely that the incorporation of elements into the cristobalite structure in co-doped samples also dampened their ability to induce cytotoxicity, although the presence of albite and reduced cristobalite content, compared to non-doped samples, may also have contributed to a decrease in toxicity (see below). Cristobalite in co-doped samples contained between 1 and 4 oxide wt% Al + Na, where the Al + Na content in cristobalite increased with increased doping. No reduction in cytotoxicity was observed for samples doped with 2 oxide wt% Al + Na, which corresponds with < 1 oxide wt% Al in its structure, compared to non-doped samples. However, samples doped with > 3 oxide wt% Al + Na (> 1.4 oxide wt% Al in their structure) had diminished cytotoxicity. Therefore, we see an empirical threshold of ~1 oxide wt% Al in the cristobalite structure, above which cristobalite cytotoxicity is reduced for these synthetic samples. This same trend was not seen for the haemolytic potential of the samples, where the amount of dopant does not appear to influence the extent of haemolysis in Al + Na

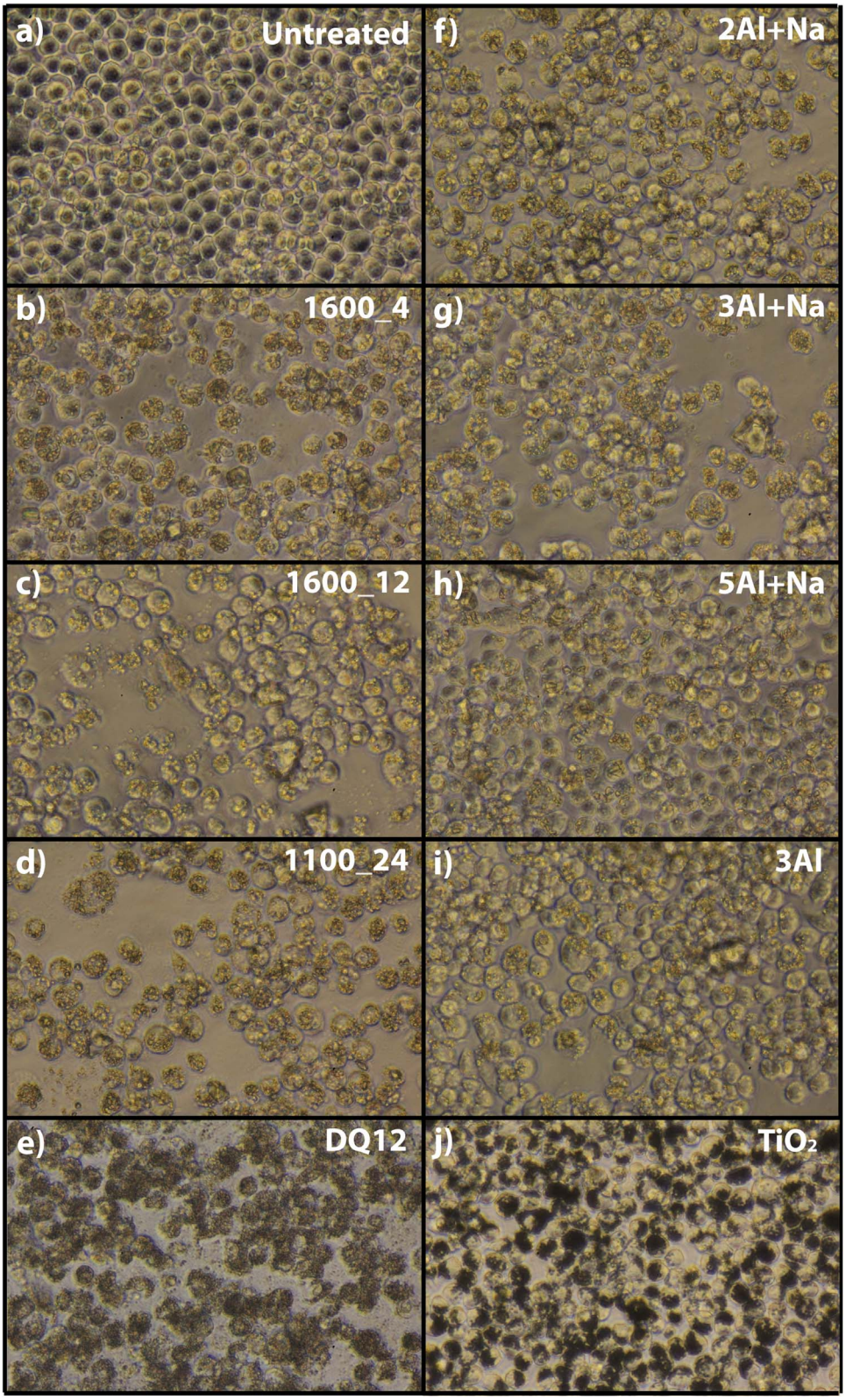

Fig. 7. Light microscopy images of J774 macrophages post-24 h treatment with 500 μg/ml samples. a) untreated cells, **b-c)** non-doped cristobalite, **d)** non-doped tridymite, **e)** DQ12 quartz, **f-i)** doped cristobalite, and **j)** TiO_2 (× 32 magnification). In **c, d** and **e,** particles that have not been engulfed are present.

doped samples, suggesting similar surface chemistry among these samples.

Elements incorporated structurally will be present at the surface of the particle, as well as internally. Al treatment of the quartz surface decreases its cytotoxic potency, ability to induce inflammatory indicators, and its haemolytic potency (Duffin et al., 2001; Nolan et al., 1981). It has been suggested that an Al treatment would bind to silanols (a surface functional group with the connectivity Si–O–H) on the silica surface, replacing H^+ and, thereby, prevent the adsorption of cell membrane components to the silica surface (Fubini, 1998). Pavan et al. (Pavan et al., 2013, 2014; Pavan and Fubini, 2016) have shown that the distribution of silanols on the silica surface affects its haemolytic and inflammatory potency, and Turci et al. (2016) have also shown that the silanol distributions on fractured crystal faces are a key factor in

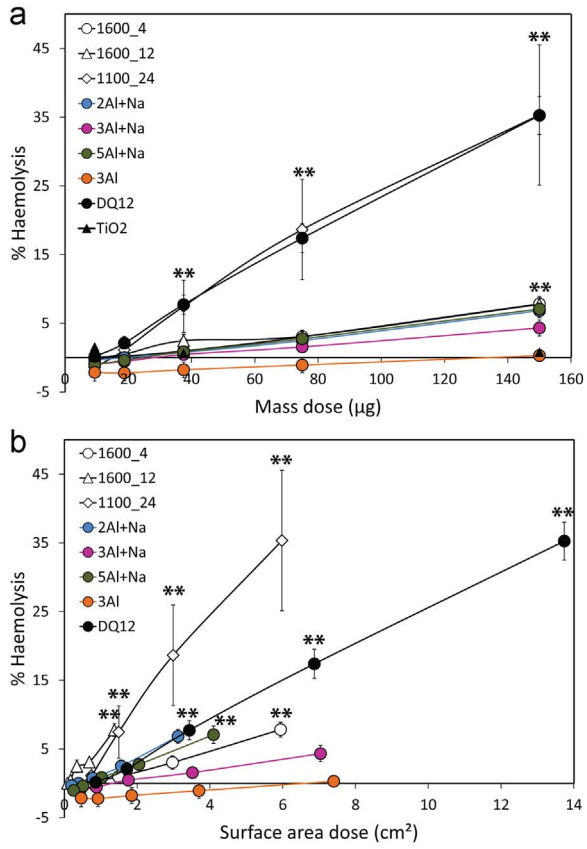

Fig. 8. Haemolytic potential of crystalline silica samples to sheep red blood cells. Haemolysis as a percentage of a positive (Triton X) and untreated control for red blood cells treated with 62–1000 µg/ml sample concentrations for 1 h, presented by **a)** mass dose, and **b)** surface area dose. Error bars represent standard error (n = 4). ** p = < 0.01 difference from untreated control.

membrane damage. Therefore, structural substitution of Al for Si ions would alter the distribution and abundance of these silanols, affecting the silica surface-cell interactions and, therefore, haemolytic potential and cytotoxicity, as seen here.

It is possible that, as structural impurities were seen throughout the cristobalite crystals, and the ameliorating effect on cristobalite cytotoxicity was sustained up to 48 h, the effect of impurities here will be long-term. However, in vivo studies would be needed to confirm if the ameliorating effect of Al impurities can be sustained in the lung.

The data suggest that co-doping with Al + Na might be less effective at decreasing cytotoxicity or haemolytic potential compared to Al-only doping. We hypothesise that Na in the structure may somehow hinder the ability of Al to suppress reactivity. The mechanism behind this should be the focus of future work, as the presence of both Al and Na is more representative of natural or industrially-occurring cristobalite. However, the explanation may lie in the presence and effect of the accessory minerals in the co-doped samples (discussed below) and it will be challenging to separate the two effects as, in this study, we were unable to grow only cristobalite in co-doped samples (of > 2 wt% Al + Na).

4.2.2. Presence of other mineral phases

The presence of other mineral phases was not anticipated here, but has been considered to have an ameliorating effect on crystalline silica toxicity in mixed dusts, such as diatomaceous earth, volcanic ash and coalmine dust, by altering or masking the surface of the crystalline silica or by interacting with the silica particle once inhaled (Donaldson and Borm, 1998; Ghiazza et al., 2009; Horwell et al., 2012; Nattrass et al., 2015). Therefore, the presence of Al and Na-rich phases (albite and an unidentified Al- and Na-rich phase) may also have impacted the toxicity of cristobalite, here. Feldspars are generally considered to have low toxicity (e.g., Housley et al., 2002) so it is unlikely that albite would contribute to the toxicity of these samples, but it may have masked the surface of the crystalline silica (if still adhered to the cristobalite after pulverisation), thereby reducing its toxic potency. However, as albite was observed in Al + Na doped samples but was barely detected in the Al-only doped sample and, as discussed, the Al-only doped sample was the least reactive, it cannot be the sole cause for the decreased reactivity of doped samples.

4.2.3. Crystalline silica polymorph and abundance

Doping caused variation in the crystalline silica polymorph produced under the same treatment conditions; the non-doped sample heated to 1100 °C produced predominantly tridymite (1100_24), whereas doped samples treated at that temperature produced cristobalite. This was expected because synthesis was undertaken within the tridymite stability field (Deer et al., 2013), but was considered an important comparison nonetheless. Studies of tridymite toxicity are limited, but its toxic potential has been suggested to be similar to cristobalite, based on their similar structure (Smith, 1998). This hypothesis is supported by Marks et al. (1956), who showed no difference between cristobalite and tridymite toxicity towards guinea pig cells in vitro. However, intratracheally-injected tridymite into rats was shown to be more potent at initiating fibrosis than quartz or cristobalite (King et al., 1953). This suggests that tridymite toxicity is variable, as with quartz and cristobalite, and is in agreement with a study by Mossman and Glenn (2013), which showed no difference, overall, between the pathogenicity of cristobalite and quartz. This suggests that surface properties of the particles are more important than the silica polymorph in determining toxicity.

In the present study, non-doped 1100_24 (tridymite) had a similar cytotoxic capacity to the non-doped cristobalites, and a similar haemolytic capacity to 1600_12 (non-doped cristobalite) based on surface area dose, suggesting similar surface reactivity between the polymorphs. However, by mass, 1100_24 was significantly more haemolytic than either the non-doped or doped cristobalite samples.

Lower cristobalite abundance was observed in the doped cristobalite samples (Table 2) compared to non-doped cristobalite. As tridymite was formed at the same treatment conditions as doped cristobalite samples (heated at 1100 °C for 24 h), it is not possible to compare crystal abundance directly between non-doped and doped samples, and it is unclear whether the reduction in crystal abundance in doped cristobalite samples compared to non-doped cristobalite (formed at 1600 °C) is due to the addition of dopants, or differences in production conditions. However, previous studies show that doping with Na (Chao and Lu, 2000) or Al (Chao and Lu, 2002a) can decrease cristobalite abundance, therefore, it is likely that doping resulted in the decreased abundance seen in doped samples here.

It is likely that the lower cristobalite abundance in doped samples contributed to their decreased cytotoxicity compared to non-doped samples. Indeed, the three samples with ~90% cristobalite (1600_4, 1600_12 and 2Al + Na) were more cytotoxic than the three samples containing ~60% cristobalite (3Al + Na, 5Al + Na and 3Al). However, haemolytic potential did not correlate with cristobalite abundance, and the greater reduction in reactivity of the Al-only sample (3Al) in both the haemolysis and LDH assays compared with the > 3 oxide wt% Al + Na doped samples, all of which contained ~60% cristobalite, highlights a dependence on additional characteristics beyond crystal abundance, as discussed above.

4.3. The effect of doping on particle uptake

Al lactate treatment has been shown to decrease particle uptake by epithelial cells (Schins et al., 2002). The J774 macrophages used in the present study are considered professional phagocytes, and particle

uptake, therefore, differs from epithelial cells. Nonetheless, some particles were not engulfed by cells and this was most-commonly observed in cells treated with non-doped samples. The uptake technique used was not quantitative, however, and could be influenced by differences in the ability to visualise the different particle types by light microscopy (e.g., due to agglomeration). The similar zeta potential for all samples, standards and starting materials is possibly due to coating of the particles with proteins, as foetal bovine serum is included in the complete medium. This coating means that particle uptake is likely not affected by particle charge, however, once engulfed, this coating may be broken down and the presence of Al and Na at the surface of doped samples may then affect particle reactivity in the cell. Therefore, unlike the aforementioned study using epithelial cells, the observation of particles that were not engulfed by macrophages could be attributed to release from dead cells. Since cytotoxicity was greater for the non-doped samples, this might explain why these particles could be visualised more easily outside of cells.

4.4. The effect of doping on pro-inflammatory mediators

TNF-α is involved in the pathway of silica pathogenicity (Piguet et al., 1990). Al treatment of quartz has been shown to decrease its ability to induce inflammatory cytokine (MIP-2) release, and prevent quartz induction of NF-κB activation (Duffin et al., 2001), which can lead to the inhibition of TNF-α production (Chen et al., 1995; Gozal et al., 2002; Rojanasakul et al., 1999). However, in the present study, the synthesised non-doped samples did not affect TNF-α production. The lack of TNF-α production in cells treated at sub-lethal concentrations suggests that these samples do not have the ability to cause inflammation via the TNF-α pathway previously observed for quartz (Chen et al., 1995; Rojanasakul et al., 1999), and that TNF-α is not involved in the observed cytotoxicity. Previously, Gozal et al. (2002) showed that silica can induce apoptosis in cells with no increase in TNF-α production. TNF-α production by macrophages, and by triple-cell co-cultures including macrophages, has also been shown to be low in cristobalite-rich diatomaceous earth samples (Nattrass et al., 2015), and cristobalite-rich volcanic ash (Damby et al., 2015; Tomašek et al., 2016).

4.5. Other factors affecting reactivity

Median particle size did not vary much amongst the samples and particle size distributions were similar for most samples, although non-doped samples were slightly coarser, whereas surface area ranged from 1 to 5 m^2/g in the crystallised samples. No correlation between surface area and particle size was observed, possibly due to the presence of pore spaces as, during heat treatment, water and N_2 are removed, potentially leaving pores (Fig. 1). Alternatively, as particle size is measured in solution, it is possible that there was preferential aggregation of some samples compared to others, although all samples were sonicated to try to prevent aggregation. The bi- or multi-model particle size distributions are likely due to the presence of amorphous material, which has a lower hardness and is more easily milled to smaller particle sizes than crystalline material. Differences in surface area or particle size, alone, do not explain differences in observed cytotoxicity or haemolytic potential.

4.6. Implications for the toxicity of natural and industrial cristobalite and regulation

Findings from this study suggest that modification of cristobalite through the introduction of structural impurities, can reduce reactivity in comparison to pure cristobalite. The findings add weight to the hypothesis, posed by Horwell et al. (2012) and Nattrass et al. (2015), that the low reactivity of diatomaceous earth and volcanic cristobalite, in vitro, is controlled by the presence of both 'inherent characteristics' and 'external factors', as suggested by the working group of the International Agency for Research on Cancer, in their recognition that crystalline silica can be variably hazardous (IARC, 1997).

Doping with Al, alone, has a relatively clear effect in reducing the potential toxicity of cristobalite, with additional Na impurities appearing to lessen that effect. However, co-doping with Al + Na is more representative of the composition of natural and industrial-related cristobalite, which has never been observed to contain only Al (Horwell et al., 2012; Nattrass et al., 2015).

That crystalline silica has variable toxicity is well established (Donaldson and Borm, 1998). However, regulations, including occupational exposure limits (OELs) or permissible exposure limits (PELs), do not currently take into account this variability. Mostly, a single OEL value is used for quartz and cristobalite although, sometimes, cristobalite is given a lower OEL (i.e. more stringent) than quartz (NIOSH, 2002). However, this is based on outdated understanding, and we propose that the crystal purity and the purity of the dust, itself, in terms of crystalline silica content, are extremely important in determining potential toxicity. Therefore, it may be more appropriate to set OELs based on knowledge of the characteristics of the crystalline silica involved in the occupational exposure.

Further, hazard management responses to cristobalite exposure post volcanic eruption may be impacted by this and future research. During the 1995–2011 Soufrière Hills eruption, communities were frequently exposed to cristobalite-rich volcanic ash (Horwell et al., 2014; Baxter et al., 1999, 2014) in quantities exceeding the American Conference of Government Industrial Hygienists' OELs for cristobalite (Searl et al., 2002). However, a quantitative risk assessment of the likelihood of individuals developing silicosis showed that the ash could be regarded as a 'mixed dust' of low to moderate toxicity (Hincks et al., 2006). In future eruptions, we envisage that tailored environmental exposure limits could be set, based upon a more robust knowledge of the structure-toxicity relationship for cristobalite-rich volcanic ash (Horwell et al., 2012) in lieu of clinical studies on silicosis development, which has never yet been documented in volcanic settings (Horwell and Baxter, 2006).

5. Conclusions

Crystalline silica toxicity is variable and it has been hypothesised that inherent and external impurities can both dampen and augment cristobalite toxicity. Here, doping synthetic silica with Al or co-doping with Al and Na, pre-crystallisation, led to an apparent decrease in cristobalite cytotoxicity and haemolytic potential compared to non-doped samples. The inhibition of cristobalite-induced reactivity by Al-only doping was attributed to structurally-substituted Al. The decreased toxicity of co-doped samples compared to non-doped samples was also partially attributed to structural Al, however, the decrease in cristobalite abundance that resulted from co-doping as well as the presence of other minor aluminosilicates (albite and an unidentified phase) in these samples may also moderate this effect. Neither non-doped nor doped samples induced TNF-α production, therefore, the role of structural impurities in inflammatory processes could not be discerned.

It has previously been hypothesised that Al and Na substitutions in volcanic and diatomaceous earth cristobalite may dampen their toxicity (Horwell et al., 2012; Nattrass et al., 2015). It is shown here that these substitutions may reduce cristobalite toxicity and, therefore, are likely to contribute to dampening the toxicity of cristobalite-rich mixed-phase dusts. These findings have implications for the setting of occupational and environmental exposure limits for crystalline silica, which currently do not account for inherent characteristics which may render cristobalite dusts much less toxic than predicted by laboratory standards.

Declarations

Ethics approval and consent to participate

Not applicable.

Consent for publication

Not applicable.

Availability of data and materials

The datasets used and/or analysed during the current study available from the corresponding author on reasonable request.

Competing interests

The authors declare that they have no competing interests.

Funding

The authors acknowledge IMA Europe and Durham University as the primary funders of this study and support provided by Horwell's NERC Postdoctoral Research Fellowship (Grant no. NE/C518081/2). DED was supported by ERC Advanced Investigator Grant no. 247076 (EVOKES).

Authors' contributions

CN designed the study, performed physicochemical analyses at Durham University and in vitro toxicology assays at Heriot-Watt University, and drafted the manuscript. CJH conceived and designed the study, and supervised CN. DED advised on study outcomes, performed electron microprobe analyses, and helped with further physicochemical analyses. DB participated in in vitro assays. VS and DB participated in the design of the study and VS supervised CN. All authors helped draft the manuscript, read and approved the final version.

Acknowledgements

Thanks to Nick Marsh, University of Leicester, for XRF analyses and to Leon Bowen, Durham GJ Russell Microscopy Facility, for assistance with SEM and EDS analyses. Thanks to Ian Chaplin for assistance with sample preparation, Kathryn Melvin, Gary Oswald and David Johnson for technical assistance with laser diffraction, XRD and BET analyses, respectively. Thanks to Professor Damian Hampshire and Mark Raine for use of the high temperature furnace and initial input to experimental set-up. Thanks to the Nano-Safety Group at Heriot-Watt University for technical advice regarding the toxicology assays, and Nilesh Kanase for performing WST-1 assays.

Appendix A. Supplementary material

Supplementary data associated with this article can be found in the online version at http://dx.doi.org/10.1016/j.envres.2017.07.054.

References

Barrett, E.G., Johnston, C., Oberdörster, G., Finkelstein, J.N., 1999. Antioxidant treatment attenuates cytokine and chemokine levels in murine macrophages following silica exposure. Toxicol. Appl. Pharmacol. 158, 211–220.

Batchelder, M., Cressey, G., 1998. Rapid, accurate phase quantification of clay-bearing samples using a position-sensitive X-ray detector. Clays Clay Miner. 46, 183–194.

Baxter, P.J., Bonadonna, C., Dupree, R., Hards, V.L., Kohn, S.C., Murphy, M.D., Nichols, A., Nicholson, R.A., Norton, G., Searl, A., Sparks, R.S.J., Vickers, B.P., 1999. Cristobalite in volcanic ash of the Soufriere Hills Volcano, Montserrat, British West Indies. Science 283, 1142–1145.

Baxter, P.J., Searl, A.S., Cowie, H.A., Jarvis, D., Horwell, C.J., 2014. Chapter 22 Evaluating the Respiratory Health Risks of Volcanic Ash at the Eruption of the Soufrière Hills Volcano, Montserrat, 1995 to 2010. 39. Geological Society, London, Memoirs, pp. 407–425.

Bye, E., Davies, R., Griffiths, D.M., Gylseth, B., Moncrieff, C.B., 1984. In vitro cytotoxicity and quantitative silica analysis of diatomaceous earth products. Br. J. Ind. Med. 41, 228–234.

Carpenter, M.A., Salje, E.K.H., Graeme-Barber, A., 1998. Spontaneous strain as a determinant of thermodynamic properties for phase transitions in minerals. Eur. J. Mineral. 10, 621–691.

Chao, C.H., Lu, H.Y., 2000. Crystallization of Na2O-doped colloidal gel-derived silica. Mater. Sci. Eng. a-Struct. Mater. Prop. Microstruct. Process. 282, 123–130.

Chao, C.H., Lu, H.Y., 2002a. Beta-Cristobalite stabilization in (Na2O + Al2O3)-added silica. Metall. Mater. Trans. a-Phys. Metall. Mater. Sci. 33, 2703–2711.

Chao, C.H., Lu, H.Y., 2002b. Stress-induced beta - > alpha-cristobalite phase transformation in (Na2O + Al2O3)-codoped silica. Mater. Sci. Eng. a-Struct. Mater. Prop. Microstruct. Process. 328, 267–276.

Checkoway, H., Heyer, N.J., Demers, P.A., Breslow, N.E., 1993. Mortality among workers in the diatomaceous earth industry. Br. J. Ind. Med. 50, 586–597.

Chen, F., Sun, S.C., Kuh, D.C., Gaydos, L.J., Demers, L.M., 1995. Essential role of NF-κB activation in silica-induced inflammatory mediator production in macrophages. Biochem. Biophys. Res. Commun. 214, 985–992.

Cherry, N.M., Burgess, G.L., Turner, S., Mcdonald, J.C., 1998. Crystalline silica and risk of lung cancer in the potteries. Occup. Environ. Med. 55, 779–785.

Cullen, R.T., Jones, A.D., Miller, B.G., Tran, C.L., Davis, J.M.G., Donaldson, K., Wilson, M., Stone, V., Mrgan, A., 2002. Toxicity of volcanic ash from Montserrat. Institute of Occupational Medicine, Edinburgh (IOM TM/02/01).

Cullen, R.T., Vallyathan, V., Hagen, S., Donaldson, K., 1997. Protection by iron against the toxic effects of quartz. Ann. Occup. Hyg. 41, 420–425.

Damby, D., Duewell, P., Horwell, C.J., Baxter, P.J., Kueppers, U., Schnurr, M., Dingwell, D.B., 2015. Volcanic ash activates the NLRP3 inflammasome in macrophages in vitro. Goldschmidt Abstracts, 648.

Damby, D.E., 2012. From Dome to Disease: The Respiratory Toxicity of Volcanic Cristobalite. Durham University, Durham, UK.

Damby, D.E., Llewellin, E.W., Horwell, C.J., Williamson, B.J., Najorka, J., Cressey, G., Carpenter, M., 2014. The [alpha]-[beta] phase transition in volcanic cristobalite. J. Appl. Crystallogr. 47.

Damby, D.E., Murphy, F.A., Horwell, C.J., Raftis, J., Donaldson, K., 2016. The in vitro respiratory toxicity of cristobalite-bearing volcanic ash. Environ. Res. 145, 74–84.

Deer, W.A., Howie, R.A., Zussman, J., 2013. An Introduction to the Rock-forming Minerals. Mineralogical Society of Great Britain & Ireland.

Dollberg, D.D., Bolyard, M.L., Smith, D.L., 1986. Chapter 6: Evaluation of physical health effects due to volcanic hazards: crystalline silica in Mount St. Helens volcanic ash. Am. J. Public Health 76, 53–58.

Donaldson, K., Borm, P.J.A., 1998. The quartz hazard: a variable entity. Ann. Occup. Hyg. 42, 287–294.

Duffin, R., Gilmour, P.S., Schins, R.P.F., Clouter, A., Guy, K., Brown, D.M., Macnee, W., Borm, P.J., Donaldson, K., Stone, V., 2001. Aluminium lactate treatment of DQ12 quartz inhibits its ability to cause inflammation, chemokine expression, and nuclear factor-κB activation. Toxicol. Appl. Pharmacol. 176, 10–17.

Engh, K.R., 2000. Diatomite. Kirk-Othmer Encyclopedia of Chemical Technology. John Wiley & Sons, Inc.

Fubini, B., 1998. Surface chemistry and quartz hazard. Ann. Occup. Hyg. 42, 521–530.

Fubini, B., Bolis, V., Cavenago, A., Volante, M., 1995. Physicochemical properties of crystalline silica dusts and their possible implication in various biological responses. Scand. J. Work, Environ. Health 21 (suppl 2), s9–s14.

Ghiazza, M., Gazzano, E., Bonelli, B., Fenoglio, I., Polimeni, M., Ghigo, D., Garrone, E., Fubini, B., 2009. Formation of a vitreous phase at the surface of some commercial diatomaceous earth prevents the onset of oxidative stress effects. Chem. Res. Toxicol. 22, 136–145.

Gozal, E., Ortiz, L.A., Zou, X., Burow, M.E., Lasky, J.A., Friedman, M., 2002. Silica-induced apoptosis in murine macrophage: involvement of tumor necrosis factor-alpha and nuclear factor-kappaB activation. Am. J. Respir. Cell Mol. Biol. 27, 91–98.

Greenberg, M.I., Waksman, J., Curtis, J., 2007. Silicosis: a review. Dis. Mon. 53, 394–416.

Harber, P., Dahlgren, J., Bunn, W., Lockey, J., Chase, G., 1998. Radiographic and spirometric findings in diatomaceous earth workers. J. Occup. Environ. Med. 40, 22–28.

Hincks, T.K., Aspinall, W.P., Baxter, P.J., Searl, A., Sparks, R.S.J., Woo, G., 2006. Long term exposure to respirable volcanic ash on Montserrat: a time series simulation. Bull. Volcanol. 68, 266–284.

Horwell, C., Baxter, P., 2006. The respiratory health hazards of volcanic ash: a review for volcanic risk mitigation. Bull. Volcanol. 69, 1–24.

Horwell, C., Williamson, B., Donaldson, K., LE Blond, J., Damby, D., Bowen, L., 2012. The structure of volcanic cristobalite in relation to its toxicity; relevance for the variable crystalline silica hazard. Part. Fibre Toxicol. 9, 44.

Horwell, C., Williamson, B., Llewellin, E., Damby, D., Blond, J., 2013. The nature and formation of cristobalite at the Soufrière Hills volcano, Montserrat: implications for the petrology and stability of silicic lava domes. Bull. Volcanol. 75, 1–19.

Horwell, C.J., Hillman, S.E., Cole, P.D., Loughlin, S.C., Llewellin, E.W., Damby, D.E., Christopher, T.E., 2014. Chapter 21 Controls on Variations In Cristobalite Abundance in Ash Generated by the Soufrière Hills Volcano, Montserrat in the Period 1997 to 2010. 39. Geological Society, London, Memoirs, pp. 399–406.

Housley, D.G., Berube, K.A., Jones, T.P., Anderson, S., Pooley, F.D., Richards, R.J., 2002. Pulmonary epithelial response in the rat lung to instilled Montserrat respirable dusts and their major mineral components. Occup. Environ. Med 59, 466–472.

Hughes, J., Weill, H., Checkoway, H., Jones, R., Henry, M., Heyer, N., Seixas, N., Demers, P., 1998. Radiographic evidence of silicosis risk in the diatomaceous earth industry.

Am. J. Respir. Crit. Care Med. 158, 807–814.
IARC, 1997. Silica, Some Silicates, Coal Dust and Para-aramid Fibrils. International Agency for Research on Cancer, Lyon.
ICDD, 2015. The International Centre for Diffraction Data. 2015 ed. ⟨http://www.icdd.com/⟩: The International Centre for Diffraction Data.
King, E.J., Mohanty, G.P., Harrison, C.V., Nagelschmidt, G., 1953. The action of different forms of pure silica on the lungs of rats. Br. J. Ind. Med. 10, 9–17.
Knaapen, A.M., Albrecht, C., Becker, A., Höhr, D., Winzer, A., Haenen, G.R., Borm, P.J.A., Schins, R.P.F., 2002. DNA damage in lung epithelial cells isolated from rats exposed to quartz: role of surface reactivity and neutrophilic inflammation. Carcinogenesis 23, 1111–1120.
Leung, C.C., Yu, I.T.S., Chen, W., 2012. Silicosis. Lancet 379, 2008–2018.
Marks, J., Mason, M.A., Nagelschmidt, G., 1956. A study of dust toxicity using a quantitative tissue culture technique. Br. J. Ind. Med. 13, 38.
Meldrum, M., Howden, P., 2002. Crystalline silica: variability in fibrogenic potency. Ann. Occup. Hyg. 46, 27–30.
Mossman, B.T., Glenn, R.E., 2013. Bioreactivity of the crystalline silica polymorphs, quartz and cristobalite, and implications for occupational exposure limits (OELs). Crit. Rev. Toxicol. 43, 632–660.
Nattrass, C., 2015. The Crystalline Silica Conundrum: the Effect of Impurities on the Respiratory Toxicity of Diatomaceous Earth and Synthetic Cristobalite. Durham University, Durham, UK.
Nattrass, C., Horwell, C.J., Damby, D.E., Kermanizadeh, A., Brown, D.M., Stone, V., 2015. The global variability of diatomaceous earth toxicity: a physicochemical and in vitro investigation. J. Occup. Med. Toxicol. 10, 23.
Niosh, 2002. Health Effects of Occupational Exposure to Respirable Crystalline Silica. In: SERVICES, D. O. H. A. H. (ed.).
Nolan, R.P., Langer, A.M., Harington, J.S., Oster, G., Selikoff, I.J., 1981. Quartz hemolysis as related to its surface functionalities. Environ. Res. 26, 503–520.
Park, R., Rice, F., Stayner, L., Smith, R., Gilbert, S., Checkoway, H., 2002. Exposure to crystalline silica, silicosis, and lung disease other than cancer in diatomaceous earth industry workers: a quantitative risk assessment. Occup. Environ. Med. 59, 36–43.
Park, Y.-H., Bae, H., Jang, Y., Jeong, S., Lee, H., Ryu, W.-I., Yoo, M., Kim, Y.-R., Kim, M.-K., Lee, J., Jeong, J., Son, S., 2013. Effect of the size and surface charge of silica nanoparticles on cutaneous toxicity. Mol. Cell. Toxicol. 9, 67–74.
Pavan, C., Fubini, B., 2016. Unveiling the variability of "Quartz Hazard" in light of recent toxicological findings. Chem. Res Toxicol.
Pavan, C., Rabolli, V., Tomatis, M., Fubini, B., Lison, D., 2014. Why does the hemolytic activity of silica predict its pro-inflammatory activity? Part. Fibre Toxicol. 11, 76.
Pavan, C., Tomatis, M., Ghiazza, M., Rabolli, V., Bolis, V., Lison, D., Fubini, B., 2013. In search of the chemical basis of the hemolytic potential of silicas. Chem. Res. Toxicol. 26, 1188–1198.
Peeters, P.M., Eurlings, I.M., Perkins, T.N., Wouters, E.F., Schins, R.P., Borm, P.J., Drommer, W., Reynaert, N.L., Albrecht, C., 2014. Silica-induced NLRP3 inflammasome activation in vitro and in rat lungs. Part Fibre Toxicol. 11, 58.
Perkins, T.N., Shukla, A., Peeters, P.M., Steinbacher, J.L., Landry, C.C., Lathrop, S.A., Steele, C., Reynaert, N.L., Wouters, E.F., Mossman, B.T., 2012. Differences in gene expression and cytokine production by crystalline vs. amorphous silica in human lung epithelial cells. Part Fibre Toxicol. 9, 6.
Piguet, P.F., Collart, M.A., Grau, G.E., Sappino, A.-P., Vassalli, P., 1990. Requirement of tumour necrosis factor for development of silica-induced pulmonary fibrosis. Nature 344, 245.
Rafnsson, V., Gunnarsdóttir, H., 1997. Lung cancer incidence among an Icelandic cohort exposed to diatomaceous earth and cristobalite. Scand. J. Work, Environ. Health 23, 187–192.
Rice, F.L., Park, R., Stayner, L., Smith, R., Gilbert, S., Checkoway, H., 2001. Crystalline silica exposure and lung cancer mortality in diatomaceous earth industry workers: a quantitative risk assessment. Occup. Environ. Med. 58, 38–45.
Rojanasakul, Y., Ye, J., Chen, F., Wang, L., Cheng, N., Castranova, V., Vallyathan, V., Shi, X., 1999. Dependence of NF-kappaB activation and free radical generation on silica-induced TNF-alpha production in macrophages. Mol. Cell Biochem 200, 119–125.
Schins, R.P.F., Duffin, R., Höhr, D., Knaapen, A.M., Shi, T., Weishaupt, C., Stone, V., Donaldson, K., Borm, P.J.A., 2002. Surface modification of quartz inhibits toxicity, particle uptake, and oxidative DNA damage in human lung epithelial cells. Chem. Res. Toxicol. 15, 1166–1173.
Searl, A., Nicholl, A., Baxter, P.J., 2002. Assessment of the exposure of islanders to ash from the Soufriere Hills volcano, Montserrat, British West Indies. Occup. Environ. Med. 59, 523–531.
Smith, D.K., 1998. Opal, cristobalite, and tridymite: noncrystallinity versus crystallinity, nomenclature of the silica minerals and bibliography. Powder Diffr. 13, 2–19.
Stone, V., Jones, R., Rollo, K., Duffin, R., Donaldson, K., Brown, D.M., 2004. Effect of coal mine dust and clay extracts on the biological activity of the quartz surface. Toxicol. Lett. 149, 255–259.
Tomašek, I., Horwell, C.J., Damby, D.E., Barošová, H., Geers, C., Petri-Fink, A., Rothen-Rutishauser, B., Clift, M.J.D., 2016. Combined exposure of diesel exhaust particles and respirable Soufrière Hills volcanic ash causes a (pro-)inflammatory response in an in vitro multicellular epithelial tissue barrier model. Part. Fibre Toxicol. 13, 67.
Tourmann, J.L., Kaufmann, R., 1994. Biopersistence of the mineral matter of coal mine dusts in silicotic human lungs: is there a preferential release of iron? Environ. Health Perspect. 102 (Suppl 5), S265–S268.
Turci, F., Pavan, C., Leinardi, R., Tomatis, M., Pastero, L., Garry, D., Anguissola, S., Lison, D., Fubini, B., 2016. Revisiting the paradigm of silica pathogenicity with synthetic quartz crystals: the role of crystallinity and surface disorder. Part. Fibre Toxicol. 13, 32.
Vigliani, E.C., Mottura, G., 1948. Diatomaceous earth silicosis. Br. J. Ind. Med. 5, 148–160.
Wagner, W.D., Fraser, D.A., Wright, P.G., Dobrogorski, O.J., Stokinger, H.E., 1968. Experimental evaluation of the threshold limit of cristobalite—calcined diatomaceous earth. Am. Ind. Hyg. Assoc. J. 29, 211–221.
Wilson, M.R., Stone, V., Cullen, R.T., Searl, A., Maynard, R.L., Donaldson, K., 2000. In vitro toxicology of respirable Montserrat volcanic ash. Occup. Environ. Med 57, 727–733.